

JCTC

Journal of Chemical Theory and Computation

On the Performances of the M06 Family of Density Functionals for Electronic Excitation Energies

Denis Jacquemin,^{*,†} Eric A. Perpète,[†] Ilaria Ciofini,[‡] Carlo Adamo,^{*,‡}
Rosendo Valero,^{§,⊥} Yan Zhao,^{§,||} and Donald G. Truhlar[§]

Unité de Chimie Physique Théorique et Structurale (UCPTS), Facultés Universitaires Notre-Dame de la Paix, rue de Bruxelles, 61, B-5000 Namur, Belgium, Ecole Nationale Supérieure de Chimie de Paris, Laboratoire Electrochimie et Chimie Analytique, UMR CNRS-ENSCP no. 7575, 11, rue Pierre et Marie Curie, F-75321 Paris Cedex 05, France, Department of Chemistry and Supercomputing Institute, University of Minnesota, Minneapolis, Minnesota 55455-0431, and Commercial Print Engine Lab, HP Laboratories, Hewlett-Packard Co., 1501 Page Mill Road, Palo Alto, California 94304

Received March 2, 2010

Abstract: We assessed the accuracy of the four members of the M06 family of functionals (M06-L, M06, M06-2X, and M06-HF) for the prediction of electronic excitation energies of main-group compounds by time-dependent density functional theory. This is accomplished by comparing the predictions both to high-level theoretical benchmark calculations and some experimental data for gas-phase excitation energies of small molecules and to experimental data for midsize and large chromophores in liquid-phase solutions. The latter comparisons are carried out using implicit solvation models to include the electrostatic effects of solvation. We find that M06-L is one of the most accurate local functionals for evaluating electronic excitation energies, that M06-2X outperforms BHHLYP, and that M06-HF outperforms HF, although in each case, the compared functionals have the same or a similar amount of Hartree–Fock exchange. For the majority of investigated excited states, M06 emerges as the most accurate functional among the four tested, and it provides an accuracy similar to the best of the other global hybrids such as B3LYP, B98, and PBE0. For 190 valence excited states, 20 Rydberg states, and 16 charge transfer states, we try to provide an overall assessment by comparing the quality of the predictions to those of time-dependent Hartree–Fock theory and nine other density functionals. For the valence excited states, M06 yields a mean absolute deviation (MAD) of 0.23 eV, whereas B3LYP, B98, and PBE0 have MADs in the range 0.19–0.22 eV. Of the functionals tested, M05-2X, M06-2X, and BMK are found to perform best for Rydberg states, and M06-HF performs best for charge transfer states, but no single functional performs satisfactorily for all three kinds of excitation. The performance of functionals with no Hartree–Fock exchange is of great practical interest because of their high computational efficiency, and we find that M06-L predicts more accurate excitation energies than other such functionals.

I. Introduction

Time-dependent density functional theory (TD-DFT)^{1–4} is a powerful tool for evaluating properties of electronically

excited states; its predictions are often more accurate than those that can be obtained with other schemes applicable to very large molecules.^{5–24} In addition, medium effects can be readily included in TD-DFT with the help of continuum models^{25–28} (for solvents) or of hybrid quantum mechanical and molecular mechanical (QM/MM) approaches^{29–31} (for biological environments and solid-state catalysts). However, TD-DFT, like DFT for ground electronic states, is in practice applied with approximate density functionals, since an exact functional is unavailable, and many approximate functionals have systematic deficiencies, which have made the predictions less accurate for transitions with Rydberg,^{9,17} long-

* Corresponding author e-mail: denis.jacquemin@fundp.ac.be (D.J.); carlo-adamo@enscp.fr (C.A.).

[†] Facultés Universitaires Notre-Dame de la Paix.

[‡] Ecole Nationale Supérieure de Chimie de Paris.

[§] University of Minnesota.

^{||} Hewlett-Packard Co.

[⊥] Current address: Department of Chemistry, University of Coimbra, 3004-535 Coimbra, Portugal.

range charge-transfer,^{7,17} or double-excitation^{32–34} character in the excited state than for single-excitation valence transitions. It was recently concluded that TD-DFT “still represents the best compromise between accuracy and computational effort. However, large differences in the results are found between the various functionals.”²⁴ Therefore, a well informed choice of the density functional is crucial to generating reliable results. Several extensive tests of various density functionals in the TD-DFT framework have been published; tests have been carried for main-group molecules both in the gas phase and in liquid-phase solutions.^{9,10,12,14–18,20–24} Although the most extensive tests involved more than 20 functionals,²³ the M06 family^{14,35} (M06-L,³⁶ M06,¹⁴ M06-2X,¹⁴ and M06-HF¹⁰) was too new to be included. The present contribution endeavors to fill this lacuna. As in the previous tests,^{9,10,12,14–18,20–24,37} the present results are restricted to the adiabatic linear-response formulation of TD-DFT with density functionals independent of frequency and current, and in particular the adiabatic approximation implies that the functionals developed for ground-state applications are used without change.

In addition to specific applications, the performance of the functionals of the M06 family has been systematically appraised for numerous properties including thermochemistry,^{14,38–42} reaction barriers,^{14,39,41,43,44} catalysis,^{45–48} structural features,^{14,49–52} spin-state energetics,^{49,53} vibrational frequencies and intensities,^{14,54,55} noncovalent interactions,^{14,39,50,51,56–61} and NMR shieldings and related properties.^{62–65} In most cases, the functionals of the M06 family have been found to be relatively broadly accurate and among the most accurate of their respective categories; in particular, M06-L is a very effective local functional (by which we mean a functional that depends on local values of the densities and occupied spin-orbitals (of the noninteracting reference state) and their local derivatives but does not involve an integral over all space as in the Hartree-Fock exchange operator), and the other three are very effective hybrid meta functionals (where “hybrid” denotes the inclusion of Hartree-Fock exchange, and “meta” denotes the inclusion of kinetic energy density, which depends on local derivatives of the spin-orbitals). The investigations in the TD-DFT framework are sparser, but encouraging. One set of tests¹⁰ of M06-HF and six other functionals for main-group excitation energies involved 20 valence excitations, 20 Rydberg-state excitations, and three charge transfer excitations. A later test extended this to M06-L, M06, and M06-2X and 12 older functionals; this test involved 25 valence excitations, 20 Ry excitations, and three charge transfer excitations.¹⁴ In the former study,¹⁰ M06-HF was third best for Rydberg states and best for charge transfer states, but performed poorly for valence excitations. Weighting the three classes of functionals equally, though, it was the best of the seven functionals tested. For these same excitations, weighting the three classes of excitations equally, the subsequent study¹⁴ found M06-HF was best followed by M05-2X (a precursor of M06-2X) and M06-2X. Omitting charge transfer excitations, these three functionals were respectively fifth, second, and third best, out of 16. The 16 density functionals in this study were also applied¹⁴ to five

excitation energies of neutral and cationic metal atoms (including two main-group cases); M06-L and M06 had the third and fourth lowest mean unsigned error for these. In a third systematic study,³⁹ M05-2X, the four members of the M06 family, M08-HX and M08-SO (which are later versions of M06-2X), and six older functionals were applied to nine multiplicity-changing excitation energies; M08-HX, M08-SO, and M06-2X had respectively the first, fourth, and fifth lowest mean unsigned errors, out of 13 functionals tested. One would not necessarily always want to use the functional that predicts, on average, the most accurate excitation energies; in many cases where excitation energies are important, one also needs to accurately model noncovalent interactions and/or barrier heights on the ground potential energy surface, so a broadly accurate functional with good performance for spectroscopy (even if not the best for excitation energies) may be preferable.

In order to more completely evaluate the behavior of the M06 family for the prediction of vertical excitation energies, in this paper, we will test its performance using a variety of databases, designed to include various types of transitions, ranging from valence excitations to charge transfer (CT) and Rydberg states. More specifically, we will consider five databases: two large databases taken from the previous most extensive study of functional performances²³ and three smaller databases covering also CT and Rydberg transitions.¹⁴ The two large databases are called VT and VE to denote “versus theory” and “versus experiment,” respectively.

For the VT tests, we compare TD-DFT results to accurate wave function values for the same transition; in particular, we use data proposed in the recent publications of Thiel and co-workers,^{18,32} in which multistate complete-active-space second-order perturbation theory (MS-CASPT2) and coupled cluster (CC2 and CC3) vertical transition energies were reported for 28 small molecules. This data set was also employed by Goerigk et al. in a study²¹ of doubly hybrid functionals. These VT comparisons entail little ambiguity but have the consequence that only a small and restricted group of molecules (those for which reliable benchmark results are affordable) can be examined. Therefore, in the VE tests, typical families of organic dyes (see Figure 1) encompassing different types of transitions ($n \rightarrow \pi^*$, $\pi \rightarrow \pi^*$, and $\sigma \rightarrow \pi^*$; delocalized and localized) in neutral and charged molecules have been included. Although tests against diverse experimental data are of the greatest importance for validation of theoretical approximations, potential drawbacks of such studies include the difficulty of emulating the environment of the chromophoric molecule under the experimental conditions and sometimes of assigning the transition corresponding to the reported data. One can turn the former issue, namely, environmental effects, into an advantage by using the comparisons as a combined test of density functional approximations and solvation treatments, but it does make a conclusion about the quality of individual density functionals less reliable since it is possible that the best performance could be achieved by a cancellation of errors between the description of the excited state and the treatment of environmental effects. We will minimize the latter issue by choosing molecules where we believe the assignment of the transition or transitions in

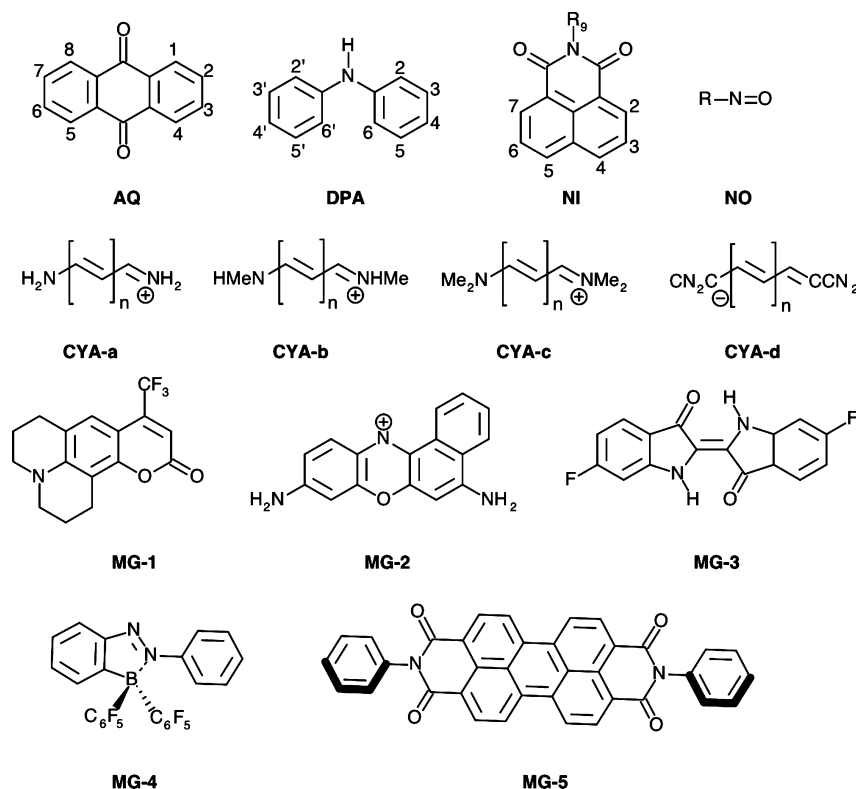


Figure 1. Molecules in the VE set.

question can be made with reasonable confidence. To organize the presentation, the VE database is broken into six subsets.

The transitions in the VT set are all single-excitation valence excitations, and the transitions in the VE set are also predominantly single-excitation valence excitations, although (as discussed below) some of them possess a partial charge transfer character. Other studies, though, showed that one does not draw the same conclusions for Rydberg states,^{10,24} which comprise a large part of the higher-energy spectrum, and for charge transfer states.¹⁰ Two of the smaller databases used here complement the VT and VE databases in that one contains 20 Rydberg-state transitions and the other contains three dominantly charge transfer excitations. These databases are denoted RES20 and CTES3, respectively.¹⁴ RES20 contains experimental data for 20 Rydberg-state transitions of N₂, CO, and HCHO. CTES3 contains theoretical data for NH₃•••F₂ at 6 Å and C₂H₄•••C₂F₄ at 8 Å and experimental data for tetracene. The other small database, VES20, contains 20 energies of valence excited states of N₂, CO, HCHO, and tetracene.^{10,14}

II. Methodology

All calculations have been performed with the *Gaussian* suite of programs, using both standard versions and development versions.^{66–69} All four functionals of the M06 family have been used: M06-HF,¹⁰ M06-L,³⁶ M06,¹⁴ and M06-2X.¹⁴ M06-L is a local meta-GGA functional. Note that, for an open-shell system, “local” denotes that it depends on the local up-spin and down-spin densities and the magnitudes of their gradients and on the local up-spin and down-spin kinetic energy densities (which depend on the self-consistent-field occupied spin-orbitals, which are themselves formally

functionals of the densities). The other three functionals are global-hybrid meta-GGA functionals, where “global-hybrid” denotes the inclusion of a certain percentage (*X*) of Hartree–Fock exchange, and “hybrid meta” denotes that the functionals depend on all the variables of a meta-GGA as well as containing Hartree–Fock exchange (which is computed from the self-consistent-field occupied spin-orbitals). The percentages of Hartree–Fock exchange are 27% for M06, 54% for M06-2X, and 100% for M06-HF. Further details and discussion of the functionals are given elsewhere.^{10,14,35–37}

II.A. Small Molecules: the VT Set. In building the present VT training set, we start with the work of Thiel and co-workers.^{18,32} In their first paper³² (which we will label ES1), they made best estimates for 104 singlets and 63 triplets, out of a total of 223 states (152 singlets and 71 triplets) considered. The best estimates are sometimes from their CC3 calculations, sometimes from their MS-CASPT2 calculations with empirical shifts based on ionization potentials and electron affinities and sometimes from the literature. In a following article¹⁸ (which we label ES2), they provided MS-CASPT2 results for 146 singlets and best estimates for 103 singlets (omitting the ¹B_{3g} state of s-tetrazine from ES1)—in 20 of these cases, they changed the ES1 best estimates, although only by small amounts. The changes are due to relativistic effects, and the mean absolute difference of the MS-CASPT2 estimates of ES1 and ES2 is only 0.01 eV. Here, as in a previous paper,²³ we use the 103 singlets for which ES2 presents best estimates (column 6 of their Table 1); these are all valence transitions (i.e., excited states that are primarily of Rydberg or charge transfer character are not included).

In order to allow consistent comparisons with the results of Thiel's group, we have employed the same basis set (TZVP) and ground-state geometry (MP2/6-31G(d), given elsewhere³² in Cartesian coordinates) that they used^{18,32} for MS-CASPT2 calculations. Note, however, that the "best theoretical estimates" do not always correspond to this geometry or basis set. To provide a comparison with a more consistent choice of geometry and basis set, we also compare to the previously reported³² MS-CASPT2/TZVP results. Although these theoretical values are not completely converged, they are plausibly close enough to the theoretical limit for vertical gas-phase transitions that they may serve as benchmarks for the present work, whose goal is to test the exchange-correlation functionals. This second comparison is not completely independent of the first since some of the best estimates are actually MS-CASPT2/TZVP results.

II.B. The VE Set. For the VE set, we followed the same procedures as in recent tests of other density functionals for dye molecules.^{16,19,70} In this approach, the ground-state structures are first optimized at the PBE0^{71,72} level using the 6-311G(d,p) basis set and the PCM ground-state solvation model²⁷ to simulate bulk liquid solvent effects. Subsequent vibrational analysis—step two—allows confirmation of whether the computed structure is a local minimum of the free energy surface. PBE0 is reasonably accurate for structural parameters of organic molecules,⁷³ and the use of the same PBE0 geometries for all of the liquid-phase tests has the effect that the comparisons of density functionals are not complicated by differences in the geometrical parameters;^{16,74} it also provides consistency with previous work.²³ In the third and final step, the vertical transition energies to the first few valence excited states are calculated using TD-DFT with each of the four density functionals and using the PCM model in a nonequilibrium absorption formulation^{26,27} for inclusion of electrostatic solvent effects. We use the 6-311+G(2d,p) basis set for the TD-DFT calculations on the VE molecules; a summary of tests showing that this basis set is adequate for the kinds of low-lying excited states under consideration here has been provided previously.²³ It is worth noting that the PCM parameters used in the calculations (such as the use of UAKS or UA0 radii or presence or absence of smoothing spheres in defining the solute cavities) vary from one family of dye to another and also depend on the functional (in part because the M06 calculations were carried out with a later version of the code), but the liquid-phase geometries are close enough to the gas-phase ones in most cases that this variation should not be significant enough to affect our conclusions.

The PCM model for electronic spectroscopy includes electrostatic effects of the medium, including the electronic polarizability of the solvent for absorption spectra, but it neglects the difference in dispersion interactions of the solvent with the ground and excited states, and it does not include hydrogen bonding effects beyond their bulk-electrostatic component and so is less accurate for protic solvents. The PCM model employed here could fail when specific solvent–solute interactions take place or when the molecular dipole moment is very different in the ground to the excited states.⁷⁵ The solvents for the VE data used in

this article are benzene (Benz), cyclohexane (CH), chloroform (CHL), dichloroethane (DCE), dichloromethane (DCM), diethyl ether (DEE), dioxane (Diox), ethanol (EtOH), heptane (Hept), hexane (Hex), methanol (MeOH), 2-methylbutane (2MPB), toluene (Tol), and water (Wat). One example of an estimate of the size of the neglected effects on excitation energies is a study of the $n \rightarrow \pi^*$ excitation of acetone in nine solvents, where dispersion effects were estimated to range from 0.07 to 0.09 eV and specific hydrogen bonding effects were estimated to range from 0 to 0.16 eV.⁷⁶ When the errors in the predicted excitation energies of the approximate density functionals are larger than these omitted effects and larger than the errors due to the uncertainties in the included bulk electrostatic effects (we do not have a quantitative estimate of the size of the uncertainties in electrostatics, but they are probably also on the order of 0.1–0.15 eV), we can draw useful conclusions about the density functionals from the comparisons to liquid-phase experimental data.

In principle, one should compare theoretical 0–0 transitions to experimental 0–0 transition energies, but since the latter are usually not available, we compare theoretical vertical transition energies to transition energies calculated from experimental^{77–106} λ_{\max} values, which entails an unknown but probably not insignificant error.^{23,107,108}

Throughout the discussion of the VT molecules, mean absolute deviations (MADs) from the experiment are calculated for the four functionals of the M06 family and compared to those for functionals not in the M06 family and sometimes also to wave function results obtained by time-dependent Hartree–Fock^{5,109} (HF) theory. The latter are calculated from results presented previously^{23,70} for the subsets of cases under discussion in each case.

The last part of the VE data set is a set of five large chromophores (MG-1 to MG-5, Figure 1) for which Goerigk et al.²¹ estimated gas-phase vertical excitation energies from experimental liquid-phase 0–0 transition energies. We compare to the liquid-phase 0–0 data for these five molecules—not to the gas-phase estimates—because medium effects are included in our approach. In particular, we applied our VE methodology to these molecules; i.e., the structures provided by Goerigk et al.²¹ have been reoptimized at the PCM-PBE0/6-311G(d,p) level and vertical (nonequilibrium) PCM-TD-DFT/6-311+G(2d,p) excitation energies have been calculated in the liquid.

In a break with the above, for five of the nitroso dyes in the VE molecule set, we will compare to gas-phase rather than liquid-phase spectra.

II.C. Rydberg and Charge Transfer Excitations. The three small databases, RES20 (Rydberg states), CTES3 (long-range charge transfer excitations), and VES20, are taken from previous work without change.^{10,14}

III. VT Benchmarks

The transition energies obtained for the VT set are listed in Table 1. Discussions of the accuracy obtained for each state by standard GGA (BP86^{110,111}),¹⁸ global hybrids (B3LYP^{112,113} and BHHLYP¹¹⁴),¹⁸ doubly hybrid functionals (B2-LYP, B2GP-LYP, B2-PLYP, and B2GP-PLYP),²¹ and range-

Table 1. VT Test Set: Gas-Phase Electronic Excitation Energies (eV) of Singlet States of Small Molecules^a

molecule	state	M06-L	M06	M06-2X	M06-HF	BE ^b	MS-CASPT2 ^c
ethene	B _{1u} (π)	7.92	7.49	7.80	7.69	7.80	8.54
butadiene	B _u (π)	5.78	5.64	5.97	6.09	6.18	6.47
	A _g (π)	6.67	6.88	7.54	7.88	6.55	6.62
hexatriene	A _g (π)	5.34	5.80	6.58	7.19	5.09	5.42
	B _u (π)	4.67	4.63	4.95	5.15	5.10	5.31
octatetraene	A _g (π)	4.42	4.96	5.76	6.41	4.47	4.64
	B _u (π)	3.97	3.99	4.29	4.53	4.66	4.70
cyclopropene	B ₁ (σ)	6.70	6.33	6.39	6.17	6.76	6.76
	B ₂ (π)	6.43	6.16	6.55	6.64	7.06	7.06
cyclopentadiene	B ₂ (π)	5.05	4.88	5.25	5.36	5.55	5.51
	A ₁ (σ)	6.40	6.53	7.07	7.69	6.31	6.31
norbonadiene	A ₂ (π)	4.82	4.78	5.15	5.24	5.34	5.34
	B ₂ (π)	5.36	5.55	6.04	6.30	6.11	6.11
benzene	B _{2u} (π)	5.41	5.30	5.57	5.77	5.08	5.04
	B _{1u} (π)	6.10	5.87	6.40	6.62	6.54	6.42
	E _{1u} (π)	7.20	6.94	7.20	7.21	7.13	7.13
	E _{2g} (π)	8.65	8.88	9.65	10.23	8.41	8.18
naphthalene	B _{3u} (π)	4.38	4.38	4.64	4.86	4.24	4.24
	B _{2u} (π)	4.24	4.28	4.73	5.08	4.77	4.77
	A _g (π)	6.11	6.13	6.55	6.94	5.87	5.87
	B _{1g} (π)	5.36	5.67	6.27	6.54	5.99	5.99
	B _{3u} (π)	5.96	5.86	6.11	6.21	6.06	6.06
	B _{2u} (π)	6.06	6.00	6.45	6.68	6.33	6.33
	B _{1g} (π)	6.36	6.17	6.66	7.42	6.47	6.47
	A _g (π)	6.87	6.89	7.67	8.08	6.67	6.67
furan	B ₂ (π)	6.29	6.03	6.37	6.47	6.32	6.39
	A ₁ (π)	6.66	6.68	7.14	7.54	6.57	6.50
	A ₁ (π)	8.43	8.09	8.40	8.40	8.13	8.17
pyrrole	A ₁ (π)	6.50	6.48	6.90	7.27	6.37	6.31
	B ₂ (π)	6.48	6.24	6.62	6.77	6.57	6.33
	A ₁ (π)	8.11	7.80	8.11	8.14	7.91	8.17
imidazole	A ⁰ (π)	6.50	6.34	6.75	6.97	6.19	6.81
	A''(n)	6.37	6.36	6.77	6.57	6.81	6.19
	A ⁰ (π)	7.05	6.94	7.39	7.72	6.93	6.93
pyridine	B ₁ (n)	4.76	4.72	4.88	4.68	4.59	5.17
	B ₂ (π)	5.51	5.40	5.66	5.84	4.85	5.02
	A ₂ (n)	4.92	5.05	5.53	6.00	5.11	5.51
	A ₁ (π)	6.30	6.09	6.61	6.83	6.26	6.39
	A ₁ (π)	7.42	7.21	7.50	7.54	7.18	7.46
	B ₂ (π)	7.39	7.18	7.48	7.57	7.27	7.27
pyrazine	B _{3u} (n)	3.90	3.87	3.99	3.80	3.95	4.12
	B _{2u} (π)	5.40	5.26	5.52	5.67	4.64	4.85
	A _u (n)	4.47	4.61	5.04	5.51	4.81	4.70
	B _{2g} (n)	5.55	5.48	5.66	5.27	5.56	5.68
	B _{1u} (π)	6.51	6.28	6.78	6.97	6.58	6.89
	B _{1g} (n)	6.13	6.39	7.15	8.13	6.60	6.41
	B _{2u} (π)	7.83	7.69	8.04	8.20	7.60	7.66
	B _{1u} (π)	7.77	7.57	7.90	7.92	7.72	7.79
pyrimidine	B ₁ (n)	4.15	4.19	4.43	4.44	4.55	4.44
	A ₂ (n)	4.40	4.51	4.92	5.12	4.91	4.80
	B ₂ (π)	5.75	5.65	5.93	6.12	5.44	5.24
	A ₁ (π)	6.58	6.39	6.89	7.10	6.95	6.63
pyridazine	B ₁ (n)	3.54	3.47	3.68	3.50	3.78	3.78
	A ₂ (n)	3.96	4.06	4.56	4.71	4.31	4.31
	A ₁ (π)	5.61	5.52	5.79	5.99	5.18	5.18
	A ₂ (n)	5.34	5.32	5.66	5.99	5.77	5.77
s-triazine	A ₁ '(n)	4.20	4.35	4.87	5.46	4.60	4.60
	A ₂ '(n)	4.43	4.46	4.70	4.73	4.66	4.66
	E''(n)	4.37	4.45	4.79	4.99	4.70	4.70
	A ₂ ⁰ (π)	6.14	6.08	6.37	6.63	5.79	5.79
s-tetrazine	B _{3u} (n)	2.11	2.07	2.28	2.20	2.29	2.29
	A _u (n)	3.20	3.36	3.89	4.27	3.51	3.51
	B _{1g} (n)	4.64	4.64	4.94	4.57	4.73	4.73
	B _{2u} (π)	5.58	5.48	5.75	5.94	4.93	4.93
	B _{2g} (n)	5.13	5.17	5.47	5.32	5.20	5.20
	A _u (n)	4.89	4.88	5.23	5.45	5.50	5.50
formaldehyde	A ₂ (n)	4.23	3.78	3.59	2.99	3.88	3.99
	B ₁ (σ)	9.19	8.67	8.66	8.16	9.10	9.14
	A ₁ (π)	10.61	10.10	9.45	9.33	9.30	9.32
acetone	A ₂ (n)	4.63	4.30	4.10	3.35	4.40	4.44
	B ₁ (σ)	8.61	8.50	8.58	8.11	9.10	9.14
	A ₁ (π)	9.05	9.00	8.91	8.96	9.40	9.32

Table 1. Continued

molecule	state	M06-L	M06	M06-2X	M06-HF	BE ^b	MS-CASPT2 ^c
<i>p</i> -benzoquinone	B _{1g} (<i>n</i>)	2.22	2.48	2.67	2.38	2.76	2.76
	A _u (<i>n</i>)	2.37	2.65	2.85	2.54	2.77	2.77
	B _{3g} (<i>π</i>)	3.61	3.78	4.25	4.74	4.26	4.26
	B _{1u} (<i>π</i>)	4.69	4.89	5.24	5.60	5.28	5.28
	B _{3u} (<i>n</i>)	4.89	5.52	6.36	6.88	5.64	5.64
	B _{3g} (<i>π</i>)	6.46	6.65	7.23	7.86	6.96	6.96
formamide	A''(<i>n</i>)	5.87	5.48	5.37	4.85	5.63	5.63
	A ⁰ (<i>π</i>)	8.02	7.90	8.69	7.68	7.39	7.39
acetamide	A''(<i>n</i>)	5.84	5.54	5.43	4.85	5.69	5.69
	A ⁰ (<i>π</i>)	7.60	7.54	7.97	7.66	7.27	7.27
propamide	A''(<i>n</i>)	5.87	5.57	5.47	4.89	5.72	5.72
	A ⁰ (<i>π</i>)	7.42	7.39	7.62	7.64	7.20	7.20
cytosine	A ⁰ (<i>π</i>)	4.50	4.74	5.03	5.24	4.66	4.67
	A''(<i>n</i>)	4.19	4.80	5.77	5.36	4.87	5.12
	A''(<i>n</i>)	4.88	5.23	5.26	5.49	5.26	5.53
thymine	A ⁰ (<i>π</i>)	5.27	5.55	5.96	6.28	5.62	5.53
	A''(<i>n</i>)	4.48	4.74	4.94	4.61	4.82	4.95
	A ⁰ (<i>π</i>)	4.93	5.05	5.33	5.50	5.20	5.06
	A''(<i>n</i>)	5.24	5.96	6.25	5.85	6.16	6.38
uracil	A ⁰ (<i>π</i>)	5.71	6.19	6.69	6.92	6.27	6.15
	A ⁰ (<i>π</i>)	6.21	6.40	6.78	7.28	6.53	6.53
	A''(<i>n</i>)	4.36	4.67	4.91	4.58	4.80	4.90
	A ⁰ (<i>π</i>)	5.10	5.25	5.51	5.65	5.35	5.23
	A''(<i>n</i>)	5.20	5.87	6.18	5.79	6.10	6.28
	A ⁰ (<i>π</i>)	5.59	6.09	6.56	7.01	6.26	6.15
adenine	A''(<i>n</i>)	5.74	6.30	6.93	6.94	6.56	6.98
	A ⁰ (<i>π</i>)	6.41	6.61	6.94	7.36	6.70	6.74
	A''(<i>n</i>)	4.64	4.90	5.38	5.67	5.12	5.19
	A ⁰ (<i>π</i>)	5.24	5.27	5.57	5.83	5.25	5.20
	A ⁰ (<i>π</i>)	4.85	5.03	5.43	5.66	5.25	5.29
	A''(<i>n</i>)	5.42	5.54	5.93	6.02	5.75	5.96

^a All density functional results use the same TZVP basis set and the MP2/6-31G(d) geometry as in ref 32. The orbital in parentheses (π , n , or σ) denotes a $\pi \rightarrow \pi^*$, $n \rightarrow \pi^*$, or $\sigma \rightarrow \pi^*$ transition, respectively. ^b The BE values are the “best estimates” from ref 18, that is, either CC3 or MS-CASPT2 calculations with empirical IPEA shifts, or are taken from the literature as specified in Table 1 of ref 18 (column 6). ^c MS-CASPT2/TZVP results from ref 18.

separated hybrids (e.g., LC-BLYP,¹¹⁵ LC- ω PBE,¹¹⁶ and CAM-B3LYP¹¹⁷)²³ have already been given in the literature, and therefore we will not discuss individual transitions in detail here; rather we will discuss typical examples.

For the polyenes (butadiene, hexatriene, and octatetraene), the energy of B_u states is always underestimated by M06-L, M06, and M06-2X, but not by M06-HF, which has the smallest average error. It is encouraging that the M06-HF estimates are more accurate than those of the doubly hybrid functionals²¹ for these cases. The A_g states are poorly described due to their significant double-excitation character. We know that ground-state systems with high multireference character are generally treated better by local exchange than Hartree–Fock exchange, and if one makes an analogy between ground states with significant multireference character and excited states with significant double-excitation character, then it is not surprising that the best results for the A_g states are obtained with M06-L, which has only local exchange. The excitation energies of these states are overestimated by the hybrid functionals with the extent of the overestimation increasing with *X*, leading, for example, to very large errors of ~ 2 eV in the M06-HF calculations on hexatriene and octatetraene.

For benzene and naphthalene, the transition energies obtained with the three hybrids usually follow the trend that a larger *X* yields larger transition energies, although the trend between M06-L and M06 is sometimes an exception. For these two aromatic compounds, the MADs from the bench-

mark values increase with *X*: 0.29 eV with M06-L, 0.33 eV with M06, 0.40 eV with M06-2X, and 0.72 eV with M06-HF.

In the heterocyclic series, the first B_{2u} state of pyrazine and the first $\pi \rightarrow \pi^*$ transition of *s*-triazine are examples of challenging states.²³ For the former, M06 (5.26 eV) is closer to the best estimate (4.64 eV) and MS-CASPT2 results (4.85 eV) than B3LYP (5.37 eV)¹⁸ or PBE0 (5.44 eV),²³ but B2-PLYP is the most accurate of all functionals examined (5.16 eV).²¹ The same ranking in accuracy is obtained for the latter case. For the 20 $n \rightarrow \pi^*$ transitions of the heterocyclic subset, the MAD (using MS-CASPT2/TZVP values as benchmarks) is 0.31 eV for M06-L, 0.26 eV for M06, 0.19 eV for M06-2X, and 0.41 eV for M06-HF. In comparison, PBE0 gives notably smaller deviations for this subset (MAD of 0.13 eV),²³ and the accuracy of doubly hybrid functionals is also superior.²¹

In the series containing ketones, aldehydes, and amines, M06 is the best performing functional of Table 1 (MAD of 0.28 eV); it provides an error similar to that of B3LYP¹⁸ and PBE0.²³

For the four nucleotide bases, which are the largest systems of the VT set, the M06 and M06-2X functionals produce similar average deviations, with MADs of 0.21 and 0.25 eV, respectively, vs the MS-CASPT2 reference. Therefore, the deviations of M06 are similar to those of B3LYP, but M06-2X is almost twice as accurate as BHLYP.

Table 2. Mean Deviations (in eV) of the Density Functional Predictions from the Best Estimates of ref 32^a

functional	X	MSD	MAD	RMSD	R ²	ref
BP86	0	0.44	0.52	0.62	0.92	22
M06-L	0	0.14 (0.18)	0.35 (0.37)	0.42 (0.47)	0.91 (0.93)	this work
B3LYP	20	0.07	0.27	0.33	0.94	22
M06	27	0.12 (0.16)	0.28 (0.31)	0.34 (0.38)	0.95 (0.95)	this work
BHLYP	50	-0.43	0.50	0.62	0.89	22
DFT/MRCI	50	0.13	0.22	0.29	0.96	22
B2-LYP	53	0.45	0.52	0.62	0.90	24 ^b
B2-PLYP	53	0.01	0.18	0.25	0.97	24 ^b
M06-2X	54	-0.23 (-0.18)	0.34 (0.35)	0.46 (0.46)	0.92 (0.92)	this work
M06-HF	100	-0.32 (-0.28)	0.55 (0.56)	0.70 (0.70)	0.83 (0.83)	this work

^a The values in parentheses are deviations from MS-CASPT2/TZVP benchmarks for the same series of states (see Table 1 for both the best estimates and MS-CASPT2/TZVP results). The MSD, MAD, and RMSD are in eV, and R² is the square of the linear correlation coefficient. ^b Note that the values listed for B2-LYP and B2-PLYP have been recalculated from the raw data of ref 21 in order to use the same standard values for all results in the whole table.

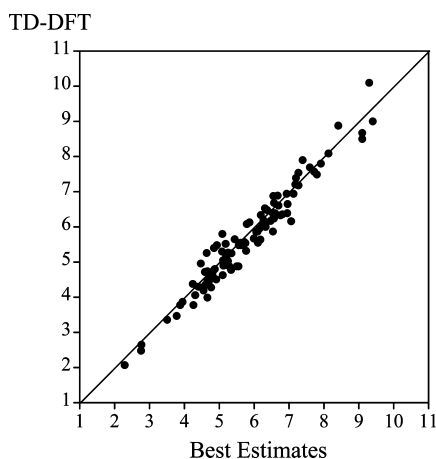


Figure 2. Comparison between TD-M06 predictions and best estimates for vertical transition energies for the full VT set (103 transitions). All values are in eV. The line at 45° corresponds to a perfect match between the two sets of values. For this data set, the MAD of M06 is 0.28 eV.

The mean signed deviations (MSDs), MADs, and root-mean-square deviations (RMSDs) obtained with the M06 family of functionals are compared to previous benchmarks in Table 2, and for the M06 functional, a graphical comparison to the best estimates is given in Figure 2. The squares of the correlation coefficients (R²) obtained by linear fitting, are also reported. Using MS-CASPT2/TZVP instead of “best estimates” as reference values leads to a small increase of the MSD (+0.04 eV) and MAD (+0.02 eV) but does not significantly affect the trends.

Irrespective of the chosen reference, M06 systematically provides the smallest errors and the largest correlation coefficient of the four functionals of the M06 family. The quality of the M06 results for the present tests is similar to that reported previously¹⁸ for B3LYP. Comparing the two functionals with X = 0, we see that M06-L surpasses BP86, with a MSD reduced by a factor of 3 and an RMSD reduced by 0.2 eV! The errors of M06-L do remain sizable, but this meta-GGA reduces the differences with respect to global hybrids, which is interesting from the point of view of the Jacob’s ladder classification¹¹⁸ of functionals since meta-GGAs are on rung 3 and hybrid GGAs and hybrid meta-GGAs are on rung 4.

Moving on to the larger percentages of Hartree–Fock exchange (larger X values), M06-2X has a similar performance to BHLYP, although they have similar percentages; the improvement is pronounced in terms of both correlation and average deviations. M06-HF produces large errors (similar to those of BP86, but with the opposite sign) and a poor correlation: it is unlikely to be of interest for calculations on excited states if only valence excitations are of interest. The DFT/MRCI scheme^{18,119} and the B2-PLYP doubly hybrid functional are significantly more accurate (although also more complicated, especially DFT/MRCI, which attempts to provide a more realistic treatment of doubly excited states) than M06, and B2-PLYP is the most accurate functional tested up to now for this set. This finding is again consistent with the Jacob’s ladder classification, since B2-PLYP is a doubly hybrid functional^{21,120} on rung 5 (the highest rung), whereas all the other functionals with nonzero X in Table 2 are on rung 4. The DFT/MRCI method in Table 2 also uses unoccupied DFT orbitals.

Figure 2 shows a graphical comparison of the M06 excitation energies to the best estimates for the full VT test set.

IV. The VE Database

The molecules belonging to the VE database can be divided into six families: the 9,10-anthraquinones (AQ, Figure 1), the (nitro)-diphenylamines (DPA, Figure 1), the 1,8-naphthalimides (NI, Figure 1), the nitroso dyes (RNO, Figure 1) the cyanines (CYA-x, Figure 1), and the large chromophores (MG-y). This latter is a subset of five dyes (MG1–MG5, Figure 1), recently studied by Goerigk et al.²¹ Table 3 collects the MSDs, MADs, RMSDs, and R² values computed using the four functionals belonging to the M06 family for all these systems, while a detailed list of the computed transition energies for the six families as well as specific discussions can be found in the Supporting Information (Tables SI.1 to Table SI.6 and related text).

IV.A. Anthraquinones (AQ), Diphenylamines (DPA), and Naphthalimides (NI): The $\pi\pi^*$ D49 Subset. The AQ, DPA, and NI families are constituted by dyes (AQ and DPA) and fluorophores (NI) largely studied both experimentally^{102,103,121–123} and theoretically,^{22,23,70,124–129,131–134} and taken together, they provided a suitable database of 49 excitation energies (30 AQ, 11 DPA, and 7 NI, respectively),

Table 3. Mean Signed (MSD) and Unsigned (MAD) Deviations (in eV) from Experimental Transitions Computed for the Molecules Belonging to the AQ, DPA, NI, RNO, Cya-x, and MG-y Families Together with the Corresponding RMSD (in eV) and R^2 Values^a

MSD				
	M06-L	M06	M06-2X	M06-HF
AQ	0.27	-0.03	-0.43	-0.84
DPA	0.45	0.13	-0.33	-0.64
NI	0.19	0.01	-0.30	-0.58
RNO	-0.21	0.20	0.39	1.08
Cya-x	-0.67	-0.55	-0.57	-0.50
MG-y	0.20	0.11	-0.13	-0.31
MAD				
	M06-L	M06	M06-2X	M06-HF
AQ	0.29	0.11	0.43	0.84
DPA	0.45	0.14	0.33	0.64
NI	0.19	0.08	0.30	0.58
RNO	0.23	0.21	0.39	1.08
Cya-x	0.67	0.55	0.57	0.50
MG-y	0.26	0.18	0.14	0.31
RMSD				
	M06-L	M06	M06-2X	M06-HF
AQ	0.33	0.13	0.43	0.85
DPA	0.47	0.15	0.35	0.67
NI	0.22	0.10	0.30	0.58
RNO	0.22	0.28	0.41	1.13
Cya-x	0.68	0.56	0.57	0.51
MG-y	0.29	0.19	0.17	0.34
R^2				
	M06-L	M06	M06-2X	M06-HF
AQ	0.89	0.96	0.98	0.97
DPA	0.91	0.95	0.91	0.78
NI	0.81	0.91	0.96	0.98
RNO	0.96	0.99	0.98	0.81
Cya-x	0.99	0.99	1.00	0.99
MG-y	0.73	0.87	0.94	0.95

^a A detailed list of computed and experimental transition energies is reported in the Supporting Information (Tables SI.1–SI.6).

all of the $\pi-\pi^*$ type, allowing for a robust benchmark to assess density functional performances for this type of transition. The MADs for the Hartree–Fock approximation and 14 density functionals for this data set (hereafter called $\pi\pi^*$ D49) are reported in Table 4. The table also gives references for the density functionals^{10,14,36,71,72,109,110,112,113,135–141} to which we compare.

In all cases, even though the members of the M06 family have different exchange and correlation potentials, as well as different values of X , the computed transition energies of the M06 family perfectly follow the percentage of Hartree–Fock exchange, i.e., $M06-L < M06 < M06-2X < M06-HF$; thus this percentage seems to be the most important parameter, as already observed for $\pi-\pi^*$ excitations.^{70,130} Three other common features for these three families of compounds can also be observed by inspection of Tables 3 and 4, in particular: (i) M06-L underestimates the transition energies but nevertheless outperforms all the previously

Table 4. Mean Unsigned Deviations (eV) from Best Estimates for the $\pi\pi^*$ D49 Data Set

functional	X^a	ref	AQ	DPA	NI	$\pi\pi^*$ D49
M06-HF	100	10	0.84	0.64	0.58	0.75
M05-2X	56	136	0.45	0.40	0.41	0.43
M06-2X	54	14	0.43	0.33	0.30	0.39
HF ^b	100	109	1.15	1.26	0.81	1.13
BMK	42	137	0.31	0.27	0.32	0.30
PBE0	25	71, 72	0.10	0.06	0.11	0.09
B98	21.98	138	0.11	0.12	0.09	0.11
M05	28	135	0.11	0.09	0.12	0.11
B3LYP	20	112, 113	0.13	0.18	0.08	0.14
M06	27	14	0.11	0.14	0.08	0.11
TPSSH	10	139	0.23	0.31	0.08	0.23
M06-L	0	36	0.29	0.45	0.19	0.31
VSXC	0	140	0.35	0.49	0.20	0.36
PBE	0	141	0.47	0.60	0.32	0.48
BLYP	0	110, 112	0.47	0.65	0.34	0.50

^a X denotes percentage of Hartree–Fock exchange. ^b This row (Hartree–Fock) is wave function theory; other rows are density functional theory.

benchmarked GGA functionals (such as PBE and BLYP) and also meta-GGAs (e.g., VSXC); (ii) the performance of M06 makes it one of the best global hybrids for this category of dyes (in the case of the $\pi\pi^*$ D49 data set, a MAD of 0.11 eV is computed for M06 as compared to 0.09 eV for PBE0 and 0.14 eV for B3LYP); (iii) M06-2X and M06-HF predict systematically higher transition energies; (iv) the MAD achieved with M06-HF is much smaller than with TD-HF (0.75 eV versus 1.13 eV for the $\pi\pi^*$ D49). Moreover, the correlation between experimental and theoretical values is usually good ($R^2 = 0.91-0.98$) for the hybrid functionals of the M06 family (with the only noteworthy exception being M06-HF for DPA) but can be significantly lower for M06-L (R^2 is only 0.81 and 0.89, in the case of NI and AQ, respectively). Finally, it is also worthwhile to remember that, in addition to the performance of the M06 functional being very close to the performances of other global hybrids that include a similar amount of Hartree–Fock exchange, fine details of substituent effects are better described by M06. For instance, M06 predicts the correct ordering for the 1,4-OH versus 1-NH₂ substitutions as well as for the 1,2-OH versus 1,8-OH patterns in the AQ family, a feat that neither PBE0 nor range-separated hybrids could achieve.⁷⁰ A more detailed discussion of computed transition energies can be found in the Supporting Information.

IV.B. Nitroso Dyes (NO18) and Cyanines (CYA13) Subsets. Due to the large separation between the $n \rightarrow \pi^*$ and $\pi \rightarrow \pi^*$ bands, nitroso derivatives (NO, Figure 1) are well-known $n \rightarrow \pi^*$ chromogens.^{121,122} The UV/vis features of NO dyes have been tackled by some of us in three previous studies of TD-DFT.^{12,23,142} The full list of the transitions (18) computed using the M06 family and a brief comment on their ordering are reported in the Supporting Information (Table SI.4 and related text).

The general trends for the nitroso dyes do not follow the pattern seen in section IV.A. For example, larger percentages of Hartree–Fock exchange generally imply smaller transition energies for nitroso dyes. Consequently, the MSDs all have the opposite sign of those for the AQ dyes (Table 3). M06 again has the smallest MAD and the largest correlation

coefficient of any member of the M06 family. The M06 MAD (0.21 eV) is significantly smaller than for its M05 precursor (0.33 eV), but larger than for PBE0 (0.08 eV). As a group, the M06 family does relatively poorly compared to other density functionals for the nitroso dyes.

Cyanine dyes are charged dyes (both anionic and cationic derivatives are considered) with highly delocalized structures. Although the four series treated in the present contribution (CYA-x, Figure 1) belong to the streptocyanine subcategory, other structures (like malachite green or nile blue) have similar electronic characteristics.⁹⁹ Due to the strong multideterminantal nature of the states of these dyes,¹⁴³ TD-DFT does not correctly predict the absolute variations of the transition energies as chain length increases. This is true with conventional hybrids,^{144,145} range-separated hybrids,^{23,130} and even doubly hybrid functionals,¹⁴⁶ though the latter provide slightly smaller absolute deviations. Table SI.5, collecting the 13 computed transitions, and Table 3 show that no functional of the M06 family succeeds in improving the usual dreadful errors, and the transition energies are still uniformly overestimated. More positively, one notes excellent correlation coefficients (Table 3) for all four functionals, just as good correlation coefficients can be obtained with other theoretical methods as well.²³ In fact, for CYA-x, the nature of the selected functional appears to be almost irrelevant, although MS-CASPT2 seems capable of mirroring the experimental measurements.¹⁴³ We will return to the classification of these transitions in section V.

IV.C. Large Chromophores (MG-y) Subset. In Table SI.6 (Supporting Information), we report the M06 family results (five transitions) for the set of large dyes recently studied by Goerigk et al.²¹ As explained in the Methodology section, estimates were made for the energies of the experimental vertical transitions, thereby attempting to remove the drawback of comparing calculated vertical transition energies to transition energies corresponding to the wavelength of maximum absorption.

Two challenging cases are discussed in more detail in the Supporting Information, and here we consider average errors for all five large chromophores, Table 3 shows the smallest errors for M06 (MAD of 0.18 eV) and M06-2X (MAD of 0.14 eV); it also shows that M06-L usually underestimates the transition energies, and M06-HF always overestimates them. For the sake of comparison, we have computed a PBE0 MAD (MSD) of 0.14 eV (0.03 eV) for the same set of five large chromophores. This is the same average error as the one obtained for a much larger set of dyes.²³ This implies that the errors obtained for low-lying excited states of organic dyes (the VE set) are smaller (on average) than for high-energy states of small molecules (see the VT set). This MAD (MSD) is substantially smaller than the one reported previously for the same functional: 0.20 eV (0.11 eV),²¹ illustrating that changes in the geometrical parameters (PBE/TZVP²¹ versus PCM-PBE0/6-311G(d,p)) and basis set (TZVP versus 6-311+G(2d,p)) substantially affect the conclusions. The most effective functional was previously²¹ found to be B2GP-PLYP, which is associated with a MAD of 0.16 eV, but this value could also be overestimated due to the testing methodology. Therefore, although we expect a non-negligible

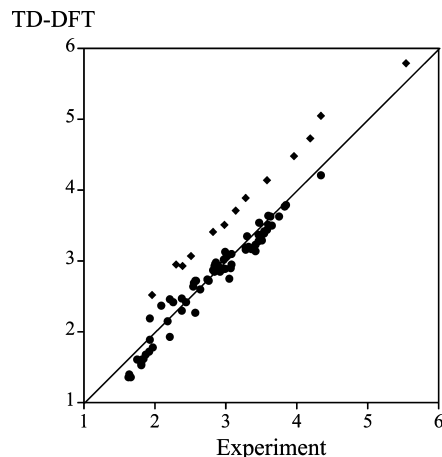


Figure 3. Comparison between experimental and theoretical (M06) transition energies (eV) for the VE set consisting of the combined $\pi\pi^*$ D49, NO18, and CYA13 data sets. The closed diamonds correspond to the CYA-x series. For this data set, the MAD of M06 is 0.20 eV.

improvement by using doubly hybrid functionals, the quantitative extent of this effect remains unsettled for large molecules.

Figure 3 shows a graphical comparison of the M06 predictions to the best estimates for the full VE data set.

V. Including Rydberg and Charge Transfer Excitations in the Assessment

The final classes of data that we consider are for Rydberg and charge transfer excitations. It is important that practical density functionals do not have large errors for these classes of excitations, because in complex molecules many transitions have some Rydberg and/or charge transfer character, and if this kind of excitation is not treated well, some components of the excited state will be misrepresented even when the predominant character of an excitation is valence-like. For example, even to treat the $\pi \rightarrow \pi^*$ excitation of ethylene correctly, it is necessary to treat valence and Rydberg states on an even-handed basis,^{147,148} and the amount of Rydberg character in a given transition can depend strongly on geometry. Charge transfer presents similar difficulties in that the extent of charge transfer covers a very wide range when one surveys a range of molecules.¹⁷ Furthermore, as mentioned at the end of section I, Rydberg states are not included in the test cases considered in both the VT and VE sets, nor is charge transfer character strongly represented in those test cases.

To illustrate the problems encountered in charge transfer states, we first consider a prototype charge transfer case, namely, the C_2H_4 molecule at a fixed distance R from a C_2F_4 molecule. The orientation is shown in Figure 4. We consider two values of R , in particular, 4 Å and 8 Å. At these distances, there is little spatial overlap of the densities of the HOMO and the LUMO, so the lowest excitation may be classified unambiguously as a charge transfer excitation (transitions that may be classified this way due to lack of overlap are called long-range charge transfer). Best estimates are obtained from the wave function calculations of Tawada et al.¹⁴⁹ and Dreuw et



Figure 4. C_2H_4 molecule at a fixed distance R from a C_2F_4 molecule. In the figure, R is 8 Å.

Table 5. Charge Transfer Excitation Energies of $C_2H_4 \cdots C_2F_4$ Separated by 4 and 8 Å and Mean Absolute Deviations from Best Estimates^a

	ref	X	4 Å	8 Å	MAD
TD-PBE0/6-31G(d)	71, 72	25	6.74	7.41	4.60
TD-PBE0/6-31+G(d)	71, 72	25	6.53	7.35	4.74
TD-PBE0/6-31++G(2d,p)	71, 72	25	6.44	7.22	4.85
TD-PBE0 ^b	71, 72	25	6.48	7.26	4.81
TD-M06-HF/6-31G(d)	10	100	10.58	12.62	0.08
TD-M06-HF	10	100	9.30	11.45	1.30
TD-M05-2X	136	56	7.62	9.32	3.21
TD-M06-2X	14	54	7.17	8.89	3.65
TD-HF ^c	109	100	10.36	12.30	0.35
TD-HFLYP	109, 112	100	11.47	12.84	0.48
TD-BMK	137	42	7.41	8.54	3.70
TD-B97-3	151	26.93	6.68	7.45	4.61
TD-B98	138	21.98	6.36	7.04	4.98
TD-M05	135	28	6.50	7.40	4.73
TD-B3LYP	112, 113	20	6.25	6.90	5.10
TD-mPW1PW	152	25	6.50	7.29	4.78
TD-X3LYP	153	21.8	6.30	7.04	5.01
TD-M06	14	27	6.77	7.21	4.69
TD-M06-L	36	0	5.43	5.70	6.11
TD-BLYP	110, 112	0	5.06	5.26	6.52
TD-CAM-B3LYP	117	19–65 ^d	7.11	9.01	3.62
TD-LC- ω PBE(20)	23	0–100 ^d	6.48	8.42	4.23
TD-LC- ω PBE	116	0–100 ^d	9.08	10.81	1.73
MS-CASPT2(4e/4o) ^{c,e}	154	100	9.15	10.09	2.06
best estimate ^f			10.72	12.63	0

^a Complex constructed taking the experimental geometries of the monomers. ^b In this table, if the basis set is not indicated, it is 6-311+G(2d,p). ^c Wave function theory (other entries are density functional theory). ^d The lower end of the range applies at zero interelectronic distance, and the upper end of the range applies at infinite interelectronic distance. ^e 4e/4o denotes four electrons in four active orbitals. These calculations were performed with MOLCAS and are based on four-state-averaged CASSCF orbitals. ^f For $R = 8.00$ Å, the best estimate comes from the SAC–CI results of Tawada et al.¹⁴⁹ The SAC–CI results are only available for $R \geq 5$ Å, but for 5 and 6 Å, the difference between the SAC–CI excitation energies and the CIS results in Figure 3 of Dreuw et al.¹⁵⁰ is constant at 0.53 eV. With this difference, the SAC–CI value at $R = 5$ Å of 11.49 eV and the CIS difference between $R = 4$ and 5 Å of 0.77 eV, we obtain a best estimate of 10.72 eV at 4 Å.

al.,¹⁵⁰ as explained in a footnote to Table 5, which also shows results for PBE0 with four basis sets, M06-HF with two, and—with one basis set—several other density func-

Table 6. Mean Absolute Deviations from Best Estimates for RES20 Database of Rydberg Excitation Energies^a

	ref	X	MAD ^a
TD-M06-HF	10	100	0.43
TD-M05-2X	136	56	0.31
TD-M06-2X	14	54	0.35
TD-HF	109	100	1.18
TD-HFLYP	109, 112	100	1.72
TD-BMK	137	42	0.35
TD-BHLLYP	114	50	0.17
TD-B97-3	151	26.93	0.78
TD-PBE0	71, 72	25	0.86
TD-B98	138	21.98	0.88
TD-M05	135	28	1.10
TD-B3LYP	112, 113	20	0.67
TD-mPW1PW	152	25	0.84
TD-X3LYP	153	21.8	0.99
TD-O3LYP	112, 155	11.61	1.55
TD-M06	14	27	1.67
TD-M06-L	36	0	1.62
TD- τ -HCTHhyb	156	15	1.08
TD- τ -HCTH	156	0	1.69
TD-TPSS	157	0	1.72
TD-BP86	110, 111	0	1.85
TD-BLYP	110, 112	0	2.00
TD-OLYP	112, 155	0	2.13
TD-SVWN5	158	0	1.77
TD-CAM-B3LYP	117	19–65	0.50
TD-LC- ω PBE(20)	23	0–100	1.14
TD-LC- ω PBE	116	0–100	0.15
TD-LC-BLYP	159	0–100	0.21
TD-LC-OLYP	23, 159	0–100	0.22
TD-LC-PBE	23, 159	0–100	0.34
TD-LC- τ -HCTH	23, 159	0–100	0.92
TD-LC-TPSS	23, 159	0–100	0.48

^a Augmented Sadlej pVTZ basis set.

tional approximations^{14,23,36,109,110,112,113,116,17,135–138,151–154} and two wave function calculations. The basis set dependence is small compared to the errors for PBE0. The MADs from the best estimates are also shown. These results are typical for long-range charge transfer excitations; only functionals with both electron correlation and 100% Hartree–Fock exchange at all values of the electronic coordinates show useful accuracy. Even the long-range corrected TD-LC- ω PBE and TD-LC- ω PBE(20) methods, which have 100% Hartree–Fock exchange in the limit of large interelectronic separation, have large errors. These results are consistent with earlier studies showing how difficult it is to get useful results for long-range charge transfer.^{10,14,17,145}

We next illustrate a similar—but not quite as dramatic—problem with Rydberg transitions. For these calculations, we used the RES20 database of 20 Rydberg-state excitation energies^{10,14} and the augmented Sadlej pVTZ basis set, and the mean unsigned errors are in Table 3. Again, we compare the results obtained with the M06 family to calculations with several other methods.^{23,71,72,109–114,116,117,135–138,151–153,155–159}

Table 6 shows that all functionals with less than 42% Hartree–Fock exchange give very poor results for Rydberg states. M06-HF, M05-2X, M06-2X, BMK, LC- ω PBE, LC-BLYP, LC-OLYP, and LC-PBE give MADs from the best results of less than 0.45 eV, but only LC- ω PBE, LC-BLYP, and LC-OLYP give MADs of 0.22 eV or less.

On the basis of the above considerations, in order to consider valence, Rydberg, and long-range charge transfer

Table 7. Mean Absolute Deviations (eV) from Best Estimates for Combined Data Sets

functional	X^a	VT103	$\pi\pi^*D49$	NO18	VES20	VES190	RES20	VRES210	CYA13	CTES3	ES226	BES226
M06-HF	100	0.55	0.75	1.08	0.71	0.67	0.39	0.64	0.50	0.09	0.63	0.54
M05-2X	56	0.39	0.43	0.51	0.37	0.41	0.31	0.40	0.66	2.42	0.44	0.53
M06-2X	54	0.34	0.39	0.39	0.34	0.36	0.35	0.36	0.57	2.46	0.40	0.50
HF ^b	100	1.05	1.13	0.15	1.08	0.99	1.18	1.01	1.08	0.99	1.01	1.05
BMK	42	0.34	0.30	0.19	0.30	0.31	0.35	0.32	0.68	3.10	0.37	0.53
PBE0	25	0.24	0.09	0.08	0.29	0.19	0.86	0.26	0.63	4.08	0.33	0.63
B98	21.98	0.25	0.11	0.07	0.24	0.20	0.92	0.26	0.61	4.25	0.34	0.65
M05	28	0.30	0.11	0.33	0.29	0.25	1.16	0.34	0.61	4.12	0.40	0.73
B3LYP	20	0.27	0.14	0.06	0.28	0.22	1.07	0.30	0.59	4.44	0.37	0.70
M06	27	0.28	0.11	0.21	0.24	0.23	1.67	0.36	0.55	4.11	0.42	0.83
TPSSh	10	0.30	0.23	0.12	0.24	0.26	1.33	0.36	0.62	4.93	0.44	0.82
M06-L	0	0.35	0.31	0.23	0.32	0.33	1.62	0.45	0.67	5.44	0.53	0.96
VSXC	0	0.39	0.36	0.17	0.27	0.35	1.64	0.47	0.65	5.63	0.55	0.98
PBE	0	0.53	0.48	0.15	0.32	0.46	1.95	0.60	0.51	5.86	0.67	1.10
BLYP	0	0.54	0.50	0.14	0.35	0.47	2.00	0.62	0.50	5.85	0.68	1.11

^a X denotes percentage of Hartree–Fock exchange. ^b This row (Hartree–Fock) is wave function theory; other rows are density functional theory.

in our assessment, results from different data sets are combined in Table 7. To this end, three small data sets (VES20, RES20, and CTES3—with all results taken from a previous paper,¹⁴ which can be consulted for details such as basis sets, geometries, and sources of accurate data) are compared to several data sets from this paper, namely, VT103, which consists of the results for the 103 excitations energies in the VT set; $\pi\pi^*D49$, which is defined above (recall that it consists of 49 $\pi \rightarrow \pi^*$ excitations of various neutral dyes); NO18, which consists of 18 $n \rightarrow \pi^*$ transitions of neutral nitroso dyes; and CYA13, which consists of 13 transitions involving highly multiconfigurational states of charged cyanines.

Table 7 does not include the five large chromophores (MG-y family, Table SI.6, Supporting Information) because we do not have results for those molecules for most of the density functionals included in Table 7. The VES190, VRES210, ES226, and BES226 columns of Table 7 are explained below.

First, we notice the difference between the trends in the CTES3 column and the VT103, $\pi\pi^*D49$, NO18, and VES20 columns of Table 7. For the long-range charge transfer states of CTES3, the errors are smallest for M06-HF, with $X = 100$, whereas for the VT103, $\pi\pi^*D49$, NO18, and VES20 databases of valence excitations, the errors are smallest for $X = 10$ –28. The CYA13 column shows a trend more in line with CTES3 than with the valence-excitation databases, although the trend is not as pronounced as for the long-range charge transfer excitations of CTES3. On the basis of this observation, we will classify the cyanine data as charge transfer excitations for the rest of this discussion.

We next defined VES190 as a database of the 190 valence excitations in VT103, $\pi\pi^*D49$, NO18, and VES20, and Table 7 shows the mean errors over all 190 data. The five best performing functionals are the ones with $X = 20$ –28, and they all have MADs in the range 0.19–0.25 eV. TPSSh, BMK, M06-L, and M06-2X are the closest trailers, with MADs in the range 0.26–0.36 eV. Adding in the Rydberg transitions of RES20 makes database VRES210 with 210 valence and Rydberg excited states; for these data, PBE0 and B98 have the best performance with MAD = 0.26 eV. M06 and M06-2X both have a MAD of 0.36 eV. Finally,

we add in the 16 charge transfer excitations of CYA13 and CTES3, and we obtain the largest data set, ES226, with 226 excited states. PBE0 and B98 remain the best performers, with MAD = 0.33–0.34 eV; the best performers in the M06 family are M06-2X and M06, with MADs of 0.40 and 0.42 eV. The 190:20:13 relative weighting of valence/Rydberg/charge-transfer excitations in ES226 (equivalent to 84:9:7) is very arbitrary. An alternative method of gaining an overall perspective would be, for example, to use a 50:25:25 weighting. We do this by first combining CYA13 and CTES3 into CTES16 and then compute a MAD for “balanced ES226” as follows:

$$\text{MAD}(\text{BES226}) = 0.50 \times \text{MAD}(\text{VES190}) + 0.25 \times \text{MAD}(\text{RES20}) + 0.25 \times \text{MAD}(\text{CTES16})$$

Such an assessment is shown in the last column of Table 7. Although it is equally as arbitrary as the raw average over the 226 molecules in ES226, it might be a more useful test when one considers a set of states having all three kinds of character. The table shows that the high- X functionals are now the best, followed by the mid- X functionals. Therefore, each potential user of the methodology must first determine whether Rydberg and/or charge transfer excitations are an important component of the transition set being studied, and the decisions on the usefulness of TD-DFT and the optimal functional depend strongly on that consideration. The bottom line is that the current situation is an unsatisfactory state of affairs because no single local or global hybrid functional is reasonably accurate for all three classes of excitation.

This is illustrated in Figure 5 where the MADs computed using the functionals belonging to the M06 family and four different combined data sets (VES190, VRES210, ES226, and BES226) are compared to the performances of other local and global hybrids functionals.

VI. Conclusions

It is important to validate practical density functional approximations in order to ascertain the reliability of their predicted electronic excitation energies. Here, we have performed benchmark calculations aimed at assaying the M06-L, M06, M06-2X, and M06-HF functionals for TD-

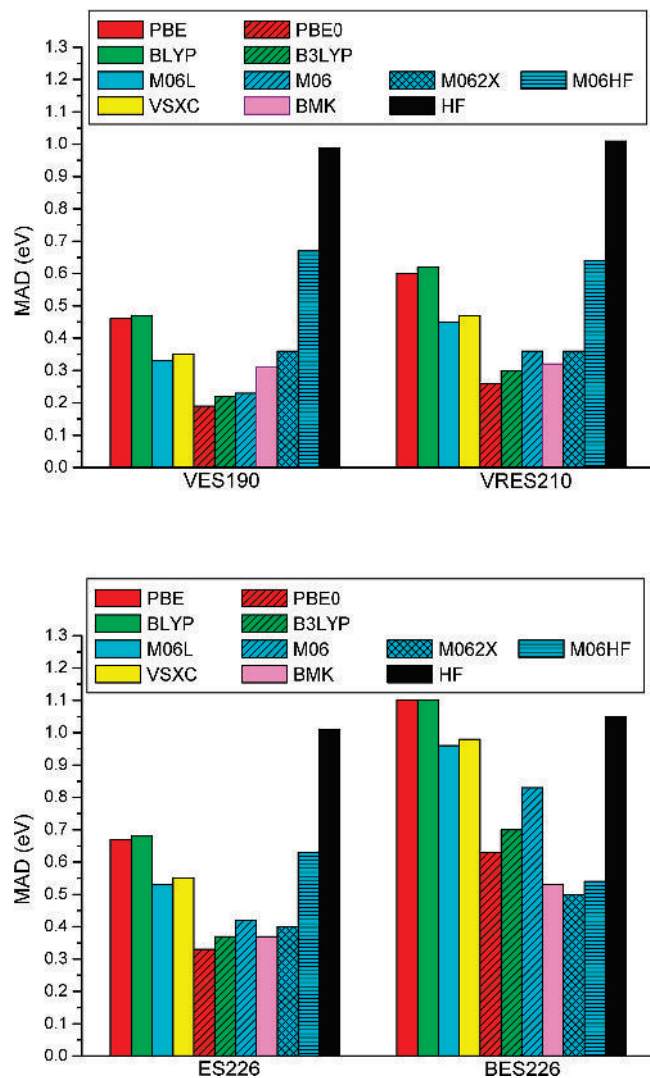


Figure 5. Computed MAD (eV) from the best estimates for combined data sets using different functionals.

DFT calculations. No functional, either one in the M06 family or any other considered functional, shows acceptable accuracy for all three of valence, Rydberg, and charge transfer excitations. Thus, we focus on valence excitations, for which the accuracy is most useful. The conclusions obtained through comparisons with theoretical benchmarks for isolated molecules and reference values inferred from experimental measurements in liquid solvents appear consistent and are as follows:

1. The M06 functional yields average deviations for valence excitations similar to those obtained with other popular hybrid functionals, namely, B3LYP and PBE0. The mean unsigned deviation (MAD) from the best estimates for the set of 190 valence excitations for which we have the most comprehensive group of comparisons set is 0.23 eV, but the deviations are significantly system-dependent. For example, the MAD is 0.39 eV for 18 $n \rightarrow \pi^*$ transitions of neutral nitroso dyes, but only 0.11 eV for a set of 49 $\pi \rightarrow \pi^*$ transitions of a variety of neutral dyes (see Tables 3–5). (In contrast, the MAD for excitations of charged cyanine dyes, which are not grouped with the valence excitations, is 0.55 eV.)

2. M06-L outperforms BP86 for the set of 103 valence-excitation benchmarks based on high-level wave function theory, and it leads to smaller errors than other meta-GGA functionals (VSXC, TPSS, and τ -HCTH) in the majority of cases. Although it tends, as do all local functionals, to underestimate the transition energies for many classes of excitation, this functional represents an improvement as compared to other local functionals.

3. Overall, M06-2X appears slightly less accurate than M06 for evaluating valence transition energies, although such a conclusion must be considered as tentative because of the lack of vibronic modeling in the majority of our VE calculations. For the VT set, the use of M06-2X improves significantly over the BHLYP estimates.

4. M06-HF is the least accurate among the four functionals of the M06 family for valence transitions. It significantly overestimates the transition energies for most $\pi \rightarrow \pi^*$ states, although the deviations are smaller than with the TD-HF approach.

In general, the trends and average errors found here for the four functionals of the M06 family are not inconsistent with expectations based on previous work.^{10,14,23}

Acknowledgment. D.J. and E.A.P. thank the Belgian National Fund for Scientific Research for their research associate and senior research associate positions, respectively. Several calculations have been performed on the Interuniversity Scientific Computing Facility (ISCF), installed at the Facultés Universitaires Notre-Dame de la Paix (Namur, Belgium), for which the authors gratefully acknowledge the financial support of the FNRS-FRFC and the “Loterie Nationale” for the convention number 2.4578.02 and of the FUNDP. The collaboration between the Belgian and French groups is supported by Wallonie-Bruxelles International, the Fonds de la Recherche Scientifique, the Ministère Français des Affaires Étrangères et Européennes, the Ministère de l’Enseignement Supérieur et de la Recherche, in the framework of Hubert Curien Partnership. The work at the University of Minnesota was supported in part by a grant to D.G.T. by the National Science Foundation (NSF). The visits of I.L. and C.A. to the University of Minnesota were supported in part by the NSF through a grant to the Institute for Mathematics and its Applications (IMA).

Supporting Information Available: Many additional details of the calculations and further discussion. This material is available free of charge via the Internet at <http://pubs.acs.org>.

References

- (1) Runge, E.; Gross, E. K. U. *Phys. Rev. Lett.* **1984**, *52*, 997.
- (2) Casida, M. E. In *Time-Dependent Density-Functional Response Theory for Molecules*; Chong, D. P., Ed.; World Scientific: Singapore, 1995; Vol. 1, pp 155–192.
- (3) Bauernschmitt, R.; Ahlrichs, R. *Chem. Phys. Lett.* **1996**, *256*, 454.
- (4) Stratmann, R. E.; Scuseria, G. E.; Frisch, M. J. *J. Chem. Phys.* **1998**, *109*, 8218.
- (5) Caricato, M.; Mennucci, B.; Tomasi, J. *J. Phys. Chem. A* **2004**, *108*, 6248.

- (6) Perdew, J. P.; Ruzsinsky, A.; Tao, J.; Staroverov, V. N.; Scuseria, G. E.; Csonka, G. I. *J. Chem. Phys.* **2005**, *123*, 62201.
- (7) Dreuw, A.; Head-Gordon, M. *Chem. Rev.* **2005**, *105*, 4009.
- (8) Jacquemin, D.; Perpète, E. A. *Chem. Phys. Lett.* **2006**, *429*, 147.
- (9) Peach, M. J. G.; Cohen, A. J.; Tozer, D. *J. Phys. Chem. Chem. Phys.* **2006**, *8*, 4543.
- (10) Zhao, Y.; Truhlar, D. G. *J. Phys. Chem. A* **2006**, *110*, 13126.
- (11) Barone, V.; Polimeno, A. *Chem. Soc. Rev.* **2007**, *36*, 1724.
- (12) Jacquemin, D.; Perpète, E. A.; Vydrov, O. A.; Scuseria, G. E.; Adamo, C. *J. Chem. Phys.* **2007**, *127*, 94102.
- (13) Ciofini, I.; Adamo, C. *J. Phys. Chem. A* **2007**, *111*, 5549.
- (14) Zhao, Y.; Truhlar, D. G. *Theor. Chem. Acc.* **2008**, *120*, 215. Unpublished errata: VES21, VRES41, CTE3, and ES44 should be VES20, VRES40, CTE3, and ES43. The final two Rydberg transitions were incorrectly labeled as valence in Table 14 of this reference, and one charge transfer transition was misassigned for M06-HF. These errors are all corrected in the present paper.
- (15) Matsuura, M.; Sato, H.; Sotoyama, W.; Takahashi, A.; Sakurai, M. *J. Mol. Struct. (THEOCHEM)* **2008**, *860*, 119.
- (16) Jacquemin, D.; Perpète, E. A.; Scuseria, G. E.; Ciofini, I.; Adamo, C. *Chem. Phys. Lett.* **2008**, *465*, 226.
- (17) Peach, M. J. G.; Benfield, P.; Helgaker, T.; Tozer, D. J. *J. Chem. Phys.* **2008**, *128*, 44118.
- (18) Silva-Junior, M. R.; Schreiber, M.; Sauer, S. P. A.; Thiel, W. *J. Chem. Phys.* **2008**, *129*, 104103.
- (19) Jacquemin, D.; Perpète, E. A.; Ciofini, I.; Adamo, C. *Acc. Chem. Res.* **2009**, *42*, 326.
- (20) Rohrdanz, M. A.; Martins, K. M.; Herbert, J. M. *J. Chem. Phys.* **2009**, *130*, 54112.
- (21) Goerigk, L.; Moellmann, J.; Grimme, S. *Phys. Chem. Chem. Phys.* **2009**, *11*, 4611.
- (22) Fabian, J. *Dyes Pigm.* **2010**, *84*, 36.
- (23) Jacquemin, D.; Wathélet, V.; Perpète, E. A.; Adamo, C. *J. Chem. Theory Comput.* **2009**, *5*, 2420.
- (24) Caricato, M.; Trucks, G. W.; Frisch, M. J.; Wiberg, K. B. *J. Chem. Theory Comput.* **2010**, *6*, 370.
- (25) Cramer, C. J.; Truhlar, D. G. *Chem. Rev.* **1999**, *99*, 2161.
- (26) Cossi, M.; Barone, V. *J. Chem. Phys.* **2001**, *115*, 4708.
- (27) Tomasi, J.; Mennucci, B.; Cammi, R. *Chem. Rev.* **2005**, *105*, 2999.
- (28) Scalmani, G.; Frisch, M. J.; Mennucci, B.; Tomasi, J.; Cammi, R.; Barone, V. *J. Chem. Phys.* **2006**, *124*, 94107.
- (29) (a) Bondar, A.-N.; Fischer, S.; Smith, J.; Elstner, M.; Suhai, S. *J. Am. Chem. Soc.* **2004**, *126*, 14668. (b) Riccardi, D.; Schaefer, P.; Yang, Y.; Yu, H.; Ghosh, N.; Prat-Resina, X.; König, P.; Li, G.; Xu, D.; Guo, H.; Elstner, M.; Cui, Q. *J. Phys. Chem. B* **2006**, *110*, 6458.
- (30) Curutchet, C.; Scholes, G. D.; Mennucci, B.; Cammi, R. *J. Phys. Chem. B* **2007**, *111*, 13253.
- (31) Jacquemin, D.; Perpète, E. A.; Laurent, A. D.; Assfeld, X.; Adamo, C. *Phys. Chem. Chem. Phys.* **2009**, *11*, 1258.
- (32) Schreiber, M.; Silva-Junior, M. R.; Sauer, S. P. A.; Thiel, W. *J. Chem. Phys.* **2008**, *128*, 134110.
- (33) Romaniello, P.; Sangalli, D.; Berger, J. A.; Sottile, F.; Molinari, L. G.; Reining, L.; Onida, G. *J. Chem. Phys.* **2009**, *130*, 44108.
- (34) Gritsenko, O. V.; Baerends, E. J. *Phys. Chem. Chem. Phys.* **2009**, *11*, 4640.
- (35) Zhao, Y.; Truhlar, D. G. *Acc. Chem. Res.* **2008**, *41*, 157.
- (36) Zhao, Y.; Truhlar, D. G. *J. Chem. Phys.* **2006**, *125*, 194101.
- (37) Świderek, K.; Paneth, P. *J. Phys. Org. Chem.* **2009**, *22*, 845.
- (38) Zhao, Y.; Truhlar, D. G. *J. Phys. Chem. A* **2008**, *112*, 1095.
- (39) Zhao, Y.; Truhlar, D. G. *J. Chem. Theory Comput.* **2008**, *4*, 1849.
- (40) Korth, M.; Grimme, S. *J. Chem. Theory Comput.* **2009**, *5*, 993.
- (41) Yang, K.; Zheng, J.; Zhao, Y.; Truhlar, D. G. *J. Chem. Phys.* **2010**, *132*, 164117.
- (42) Averkiev, B. B.; Zhao, Y.; Truhlar, D. G. *J. Mol. Catal. A* **2010**, DOI: 10.1016/j.molcata.2010.03.016.
- (43) Zheng, J. J.; Zhao, Y.; Truhlar, D. G. *J. Chem. Theory Comput.* **2007**, *3*, 569.
- (44) Zheng, J. J.; Zhao, Y.; Truhlar, D. G. *J. Chem. Theory Comput.* **2009**, *5*, 808.
- (45) Zhao, Y.; Truhlar, D. G. *J. Phys. Chem. C* **2008**, *112*, 6860.
- (46) Valero, R.; Gomes, J. R. B.; Truhlar, D. G.; Illas, F. *J. Chem. Phys.* **2008**, *129*, 124710.
- (47) Zhao, Y.; Truhlar, D. G. *J. Chem. Theory Comput.* **2009**, *5*, 324.
- (48) Valero, R.; Gomes, J. R. B.; Truhlar, D. G.; Illas, F. *J. Chem. Phys.* **2010**, *132*, 104701.
- (49) Sorokin, A.; Iron, M. A.; Truhlar, D. G. *J. Chem. Theory Comput.* **2008**, *4*, 307.
- (50) Dahlke, E. E.; Olson, R. M.; Leverentz, H. R.; Truhlar, D. G. *J. Phys. Chem. A* **2008**, *112*, 3976.
- (51) Leverentz, H. R.; Truhlar, D. G. *J. Phys. Chem. A* **2008**, *112*, 6009.
- (52) (a) Sorokin, A.; Truhlar, D. G.; Amin, E. A. *J. Chem. Theory Comput.* **2009**, *5*, 1254. (b) Mantina, M.; Valero, R.; Truhlar, D. G. *J. Chem. Phys.* **2009**, *131*, 64706. (c) Ferrighi, L.; Hammer, B.; Madsen, G. K. H. *J. Am. Chem. Soc.* **2009**, *131*, 10605.
- (53) Liao, M. S.; Watts, J. D.; Huang, M. J. *J. Chem. Theory Comput.* **2008**, *7*, 615.
- (54) Jimenez-Hoyos, C. A.; Janesko, B. G.; Scuseria, G. E. *Phys. Chem. Chem. Phys.* **2008**, *10*, 6621.
- (55) Biczysko, M.; Panek, P.; Barone, V. *Chem. Phys. Lett.* **2009**, *475*, 105.
- (56) Valdes, H.; Pluhackova, K.; Pitonak, M.; Rezac, J.; Hobza, P. *Phys. Chem. Chem. Phys.* **2008**, *10*, 2747.
- (57) (a) van Mourik, T. *J. Chem. Theory Comput.* **2008**, *4*, 1610. (b) Cao, J.; van Mourik, T. *Chem. Phys. Lett.* **2010**, *485*, 40.
- (58) Hohenstein, E. G.; Chill, S. T.; Sherrill, C. D. *J. Chem. Theory Comput.* **2008**, *4*, 1996.
- (59) Dahlke, E. E.; Olson, R. M.; Leverentz, H. R.; Truhlar, D. G. *J. Phys. Chem. A* **2008**, *112*, 3976.
- (60) Bryantsev, V. S.; Diallo, M. S.; van Duin, A. C. T.; Goddard, W. A. *J. Chem. Theory Comput.* **2009**, *5*, 1016.

- (61) Raju, R. K.; Ramarj, A.; Hillier, I. H.; Vincent, M. A.; Burton, N. A. *Phys. Chem. Chem. Phys.* **2009**, *11*, 3411.
- (62) Valero, R.; Costa, R.; Moreira, I. D. P. R.; Truhlar, D. G.; Illas, F. *J. Chem. Phys.* **2008**, *128*, 114103.
- (63) Ruiz, E. *Chem. Phys. Lett.* **2008**, *460*, 336.
- (64) Zhao, Y.; Truhlar, D. G. *J. Phys. Chem. A* **2008**, *112*, 6794.
- (65) Ribeiro, R. F.; Marenich, A. V.; Cramer, C. J.; Truhlar, D. G. *J. Chem. Theory Comput.* **2009**, *5*, 2284.
- (66) Frisch, M. J. *Gaussian 03*, revisions D.02 and E.01; Gaussian, Inc.: Wallingford, CT, 2004.
- (67) Frisch, M. J. *Gaussian DV*, revision H.01; Gaussian, Inc.: Wallingford, CT, 2008.
- (68) Zhao, Y.; Truhlar, D. G. *MN-GFM*, version 4.1; University of Minnesota: Minneapolis, MN, 2008.
- (69) Frisch, M. J.; Trucks, G. W.; Schlegel, H. B.; Scuseria, G. E.; Robb, M. A.; Cheeseman, J. R.; Scalmani, G.; Barone, V.; Mennucci, B.; Petersson, G. A.; Nakatsuji, H.; Caricato, M.; Li, X.; Hratchian, H. P.; Izmaylov, A. F.; Bloino, J.; Zheng, G.; Sonnenberg, J. L.; Hada, M.; Ehara, M.; Toyota, K.; Fukuda, R.; Hasegawa, J.; Ishida, M.; Nakajima, T.; Honda, Y.; Kitao, O.; Nakai, H.; Vreven, T.; Montgomery, J. A., Jr.; Peralta, J. E.; Ogliaro, F.; Bearpark, M.; Heyd, J. J.; Brothers, E.; Kudin, K. N.; Staroverov, V. N.; Kobayashi, R.; Normand, J.; Raghavachari, K.; Rendell, A.; Burant, J. C.; Iyengar, S. S.; Tomasi, J.; Cossi, M.; Rega, N.; Millam, N. J.; Klene, M.; Knox, J. E.; Cross, J. B.; Bakken, V.; Adamo, C.; Jaramillo, J.; Gomperts, R.; Stratmann, R. E.; Yazyev, O.; Austin, A. J.; Cammi, R.; Pomelli, C.; Ochterski, J. W.; Martin, R. L.; Morokuma, K.; Zakrzewski, V. G.; Voth, G. A.; Salvador, P.; Dannenberg, J. J.; Dapprich, S.; Daniels, A. D.; Farkas, Ö.; Foresman, J. B.; Ortiz, J. V.; Cioslowski, J.; Fox, D. J. *Gaussian 09*, Gaussian, Inc., Wallingford CT, 2009.
- (70) Jacquemin, D.; Perpète, E. A.; Scuseria, G. E.; Ciofini, I.; Adamo, C. *J. Chem. Theory Comput.* **2008**, *4*, 123.
- (71) Adamo, C.; Barone, V. *J. Chem. Phys.* **1999**, *110*, 6158.
- (72) Ernzerhof, M.; Scuseria, G. E. *J. Chem. Phys.* **1999**, *110*, 5029.
- (73) Adamo, C.; Scuseria, G. E.; Barone, V. *J. Chem. Phys.* **1999**, *111*, 2889.
- (74) Rohrdanz, M. A.; Herbert, J. M. *J. Chem. Phys.* **2008**, *129*, 34107.
- (75) Impropa, R.; Barone, V.; Scalmani, G.; Frisch, M. J. *J. Chem. Phys.* **2006**, *125*, 54103.
- (76) Li, J.; Cramer, C. J.; Truhlar, D. G. *Int. J. Quantum Chem.* **2000**, *77*, 264.
- (77) Hammick, D. L.; Lister, M. W. *J. Chem. Soc.* **1937**, 489.
- (78) Schroeder, W. A.; Wilcox, P. E.; Trueblood, K. N.; Dekker, A. O. *Anal. Chem.* **1951**, *23*, 1740.
- (79) Haszeldine, R. N.; Jander, J. *J. Chem. Soc.* **1954**, 691.
- (80) Tarte, P. *Bull. Soc. Chim. Belg.* **1954**, *63*, 525.
- (81) Jander, J.; Haszeldine, R. N. *J. Chem. Soc.* **1954**, 912.
- (82) Bugai, P. M.; Konel'skaya, V. N. *Izvest. Akad. Nauk. SSSR - Ser. Fizich.* **1954**, *18*, 695.
- (83) Labhart, H. *Helv. Chim. Acta* **1957**, *152*, 1410.
- (84) Mason, J. *J. Chem. Soc.* **1957**, 3904.
- (85) Mason, J. *J. Chem. Soc.* **1959**, 1288.
- (86) Lutskii, A. E.; Konel'skaya, V. N. *Z. Obs. Khim.* **1960**, *30*, 3773.
- (87) Bugai, P. M.; Konel'skaya, V. N.; Gol'berkova, A. S.; Bazhenova, L. M. *Z. Fizich. Khim.* **1962**, *36*, 2233.
- (88) Tabei, K.; Nagakura, S. *Bull. Soc. Chim. Japan* **1965**, *38*, 965.
- (89) Asquith, R. S.; Bridgeman, I.; Peters, A. T. *J. Soc. Dyers Colour.* **1965**, *81*, 439.
- (90) Bell, M. G. W.; Day, M.; Peters, A. T. *J. Soc. Dyers Colour.* **1966**, *82*, 410.
- (91) Asquith, R. S.; Peters, A. T.; Wallace, F. *J. Soc. Dyers Colour.* **1968**, *84*, 507.
- (92) Day, M.; Peters, A. T. *J. Soc. Dyers Colour.* **1969**, *85*, 8.
- (93) Mason, J. *J. Chem. Soc. A* **1969**, 1587.
- (94) Matsubayashi, G. E.; Takaya, Y.; Tanaka, T. *Spectrochim. Acta* **1970**, *26A*, 1851.
- (95) Weast, R. C. *Handbook of Chemistry and Physics*, 51st ed.; The Chemical Rubber Company: Cleveland, OH, 1970; p 1.
- (96) Grasselli, J. G. *Atlas of Spectral Data and Physical Constants for Organic Compounds*; The Chemical Rubber Company: Cleveland, OH, 1973; p 1.
- (97) Thomson, R. H. *Naturally Occurring Quinones*, 2nd ed.; Academic Press: London, 1971; pp 1.
- (98) Allston, T. D.; Fedyk, M. L.; Takacs, G. A. *Chem. Phys. Lett.* **1978**, *60*, 97.
- (99) Fabian, J.; Hartmann, H. *Light Absorption of Organic Colorants*; Vol. 12; Springer-Verlag: Berlin, 1980; pp 1.
- (100) Fabian, J.; Nepras, M. *Collect. Czech. Chem. Commun.* **1980**, *45*, 2605.
- (101) Csaszar, J. *Acta Phys. Chem. (Szeged)* **1987**, *33*, 11.
- (102) Green, F. J. *The Sigma-Aldrich Handbook of Stains, Dyes, and Indicators*; Aldrich Chemical Company: Milwaukee, WI, 1990; p 1.
- (103) Alexiou, M. S.; Tychopoulos, V.; Ghorbanian, S.; Tyman, J. H. P.; Brown, R. G.; Brittain, P. I. *J. Chem. Soc. Perkin Trans. 2* **1990**, 837.
- (104) Wintgens, V.; Valat, P.; Kossanyi, J.; Biczok, L.; Demeter, A.; Berces, T. *J. Chem. Soc. Faraday Trans.* **1994**, *90*, 411.
- (105) Biczok, L.; Valat, P.; Wintgens, V. *Phys. Chem. Chem. Phys.* **1999**, *1*, 4759.
- (106) Günaydin, K.; Topcu, G.; Ion, R. M. *Nat. Prod. Lett.* **2002**, *16*, 65.
- (107) (a) Parac, M.; Grimme, S. *J. Phys. Chem. A* **2002**, *106*, 6844. (b) Diercksen, M.; Grimme, S. *J. Chem. Phys.* **2004**, *120*, 3544. (c) Santoro, F.; Impropa, R.; Lami, A.; Bloino, J.; Barone, V. *J. Chem. Phys.* **2007**, *126*, 84509.
- (108) Renge, I. *J. Phys. Chem. A* **2009**, *113*, 10678–10686.
- (109) Roothaan, C. C. J. *Rev. Mod. Phys.* **1951**, *23*, 69.
- (110) Becke, A. D. *Phys. Rev. A* **1988**, *38*, 3098.
- (111) Perdew, J. P. *Phys. Rev. B* **1986**, *33*, 8822.
- (112) Lee, C.; Yang, W.; Parr, R. G. *Phys. Rev. B* **1988**, *37*, 785.
- (113) (a) Becke, A. D. *J. Chem. Phys.* **1993**, *98*, 5648. (b) Stephens, P. J.; Devlin, F. J.; Chabalowski, C. F.; Frisch, M. J. *J. Phys. Chem.* **1994**, *98*, 11623.

- (114) Becke, A. D. *J. Chem. Phys.* **1993**, *98*, 1372.
- (115) (a) Iikura, H.; Tsuneda, T.; Yanai, T.; Hirao, K. *J. Chem. Phys.* **2001**, *115*, 3540. (b) Rohrdanz, M. A.; Herbert, J. M. *J. Chem. Phys.* **2008**, *129*, 34107.
- (116) Vydrov, O. A.; Scuseria, G. E. *J. Chem. Phys.* **2006**, *125*, 234109.
- (117) Yanai, T.; Tew, D. P.; Handy, N. C. *Chem. Phys. Lett.* **2004**, *393*, 51.
- (118) Perdew, J. P.; Ruzsinszky, A.; Constantin, L. A.; Sun, J.; Csonka, G. I. *J. Chem. Theory Comput.* **2009**, *5*, 902.
- (119) Grimme, S.; Waletzke, M. *J. Chem. Phys.* **1999**, *111*, 5645.
- (120) Zhao, Y.; Lynch, B. J.; Truhlar, D. G. *J. Phys. Chem. A* **2004**, *108*, 4786.
- (121) Griffiths, J. *Colour and Constitution of Organic Molecules*; Academic Press: London, 1976; p 1.
- (122) Christie, R. M. *Colour Chemistry*; The Royal Society of Chemistry: Cambridge, UK, 1991; p 228.
- (123) Zollinger, H. *Color Chemistry, Syntheses, Properties and Applications of Organic Dyes and Pigments*, 3rd ed.; Wiley-VCH: Weinheim, Germany, 2003; p 647.
- (124) Jacquemin, D.; Preat, J.; Charlot, M.; Wathélet, V.; André, J. M.; Perpète, E. A. *J. Chem. Phys.* **2004**, *121*, 1736.
- (125) Jacquemin, D.; Preat, J.; Wathélet, V.; André, J. M.; Perpète, E. A. *Chem. Phys. Lett.* **2005**, *405*, 429.
- (126) Perpète, E. A.; Wathélet, V.; Preat, J.; Lambert, C.; Jacquemin, D. *J. Chem. Theory Comput.* **2006**, *2*, 434.
- (127) Jacquemin, D.; Assfeld, X.; Preat, J.; Perpète, E. A. *Mol. Phys.* **2007**, *105*, 325.
- (128) Jacquemin, D.; Wathélet, V.; Preat, J.; Perpète, E. A. *Spectrochim. Acta A* **2007**, *67*, 334.
- (129) Preat, J.; Laurent, A. D.; Michaux, C.; Perpète, E. A.; Jacquemin, D. *J. Mol. Struct. (THEOCHEM)* **2009**, *901*, 24.
- (130) Jacquemin, D.; Perpète, E. A.; Scalmani, G.; Frisch, M. J.; Kobayashi, R.; Adamo, C. *J. Chem. Phys.* **2007**, *126*, 144105.
- (131) Jacquemin, D.; Bouhy, M.; Perpète, E. A. *J. Chem. Phys.* **2006**, *124*, 204321.
- (132) Demeter, A.; Berces, T.; Biczok, L.; Wintgens, V.; Valat, P.; Kossanyi, J. *J. Phys. Chem.* **1996**, *100*, 2001.
- (133) Jacquemin, D.; Perpète, E. A.; Scalmani, G.; Frisch, M. J.; Ciofini, I.; Adamo, C. *Chem. Phys. Lett.* **2007**, *448*, 3.
- (134) Miao, L.; Yao, Y.; Yang, F.; Wang, Z.; Li, W.; Hu, J. *J. Mol. Struct. (THEOCHEM)* **2008**, *865*, 79.
- (135) Zhao, Y.; Truhlar, D. G. *J. Chem. Phys.* **2005**, *123*, 161103.
- (136) Zhao, Y.; Truhlar, D. G. *J. Chem. Theory Comput.* **2006**, *2*, 364.
- (137) Boese, A. D.; Martin, J. M. L. *J. Chem. Phys.* **2004**, *121*, 3405.
- (138) Schmider, H. L.; Becke, A. D. *J. Chem. Phys.* **1998**, *108*, 9624.
- (139) Staroverov, V. N.; Scuseria, G. E.; Tao, J.; Perdew, J. P. *J. Chem. Phys.* **2003**, *119*, 12129.
- (140) Van Voorhis, T.; Scuseria, G. E. *J. Chem. Phys.* **1998**, *109*, 400.
- (141) Perdew, J. P.; Burke, K.; Ernzerhof, M. *Phys. Rev. Lett.* **1996**, *77*, 3865.
- (142) Jacquemin, D.; Perpète, E. A. *Chem. Phys. Lett.* **2006**, *420*, 529.
- (143) Schreiber, M.; Bub, V.; Fülischer, M. P. *Phys. Chem. Chem. Phys.* **2001**, *3*, 3906.
- (144) Guillaumont, D.; Nakamura, S. *Dyes Pigm.* **2000**, *46*, 85.
- (145) Fabian, J. *Theor. Chem. Acc.* **2001**, *106*, 199.
- (146) Grimme, S.; Neese, F. *J. Chem. Phys.* **2007**, *127*, 154116.
- (147) Buenker, R. J.; Peyerimhoff, S. D.; Kammer, W. D. *J. Chem. Phys.* **1971**, *555*, 814.
- (148) Buenker, R. J.; Peyerimhoff, S. D. *Chem. Phys.* **1975**, *36*, 415.
- (149) Tawada, Y.; Tsuneda, T.; Yanagisawa, S.; Yanai, T.; Hirao, K. *J. Chem. Phys.* **2004**, *120*, 8425.
- (150) Dreuw, A.; Weisman, J. L.; Head-Gordon, M. *J. Chem. Phys.* **2003**, *119*, 2943.
- (151) Keal, T. W.; Tozer, D. J. *J. Chem. Phys.* **2005**, *123*, 121103.
- (152) Adamo, C.; Barone, V. *J. Chem. Phys.* **1998**, *108*, 664.
- (153) Xu, X.; Goddard, W. A., III *Proc. Natl. Acad. Sci. U.S.A.* **2004**, *101*, 2673.
- (154) Serrano-Andrés, L.; Merchán, M.; Nebot-Gil, I.; Lindh, R.; Roos, B. O. *J. Chem. Phys.* **1993**, *98*, 3151.
- (155) (a) Handy, N. C.; Cohen, A. J. *Mol. Phys.* **2001**, *99*, 403. (b) Baker, J.; Pulay, P. *J. Chem. Phys.* **2002**, *117*, 1441.
- (156) Boese, A. D.; Handy, N. C. *J. Chem. Phys.* **2002**, *116*, 9559.
- (157) Tao, J.; Perdew, J.; Staroverov, V.; Scuseria, G. *Phys. Rev. Lett.* **2003**, *91*, 146401.
- (158) (a) Slater, J. C. *Phys. Rev.* **1951**, *81*, 385. (b) Vosko, S. J.; Wilk, L.; Nusair, M. *Can. J. Phys. Can. J. Phys.* **1980**, *58*, 1200.
- (159) Tawada, Y.; Tsuneda, T.; Yanagisawa, S.; Yanai, T.; Hirao, K. *J. Chem. Phys.* **2004**, *120*, 8425.

CT100119E